https://doi.org/10.2352/ISSN.2470-1173.2020.9.IQSP-371

Prediction of Lee filter performance for Sentinel-1 SAR images

Oleksii Rubel[a], Vladimir Lukin[a], Andrii Rubel[a], Karen Egiazarian[b]
[a] National Aerospace University, 61070, Kharkiv, Ukraine;
[b] Tampere University, FIN 33101, Tampere, Finland

Abstract

Synthetic aperture radar (SAR) images are corrupted by a specific noise-like phenomenon called speckle that prevents efficient processing of remote sensing data. There are many denoising methods already proposed including well known (local statistic) Lee filter. Its performance in terms of different criteria depends on several factors including image complexity where it sometimes occurs useless to process complex structure images (containing texture regions). We show that performance of the Lee filter can be predicted before starting image filtering and which can be done faster than the filtering itself. For this purpose, we propose to apply a trained neural network that employs analysis of image statistics and spectral features in a limited number of scanning windows. We show that many metrics including visual quality metrics can be predicted for SAR images acquired by Sentinel-1 sensor recently put into operation.

Keywords: Lee filter, SAR image, performance prediction, neural network

Introduction

Radar imaging has become a useful tool to collect data from scenes of large territories [1-3]. One problem in radar imaging as well as medical imaging is the presence of intensive noise [1, 4]. This noise, which is especially intensive in synthetic aperture radar (SAR) images, is also called speckle and it is multiplicative, non-Gaussian and spatially correlated [4, 5].

In practice, it is desired to remove this specific noise, i.e., to carry out filtering (denoising, despeckling) [4-6]. However, it is not always possible, at least, without introduction of degradation of useful information [6-8]. In other words, a positive effect of speckle suppression takes place simultaneously with a negative effect of smearing of image edges and details. Depending on properties of an image, a filter used and characteristics of speckle, there can be different proportion of positive and negative effects. In case when this proportion is about 50/50, the use of despeckling is becoming unreasonable procedure [8-10].

Thus, it is important to predict the filtering performance before applying image filtering. We have demonstrated earlier [10] that such a prediction is possible for filters based on discrete cosine transform (DCT) with application to SAR images acquired by Sentinel-1 sensor. Here several aspects are worth noting. First, data provided by Sentinel-1 sensor have been already used for several important applications [11, 12]. Second, there are numerous papers dealing with estimation of image quality [13-15] including visual quality and prediction of filtering efficiency [10, 16-18]. For the corresponding methods, there is a clear tendency to apply neural networks [10, 14]. Third, it becomes more and more popular to employ visual quality metrics in analysis of image original quality and filter performance [10, 17-22]. Fourth, it has been shown that filtering efficiency can be predicted for different types of noise (additive, pure multiplicative, and, in general, signal dependent; white and spatially correlated) and for different types of filters [17].

Filtering based on DCT [10, 18] is one type of filtering used to remove speckle. Meanwhile, there are many other methods to deal with SAR image denoising and prediction of their efficiency. Thus, we have tried to design and apply a predictor based on trained neural network (NN) for the well-known Lee filter [23] that is included in many existing tools for SAR image despeckling. As an example, Sentinel-1 SAR images are considered as a potential application with the reasons given above.

Our study has two main goals. On one hand, we aim at demonstrating that our approach proposed in [10] is quite general, applicable to other despeckling methods. On the other hand, one stage of getting data for training the NN-based predictor is filtering of a rather large number of test images that shall be performed in advance. Whilst it is not a big problem for the DCT-based filter (data are obtained in a day or a few days [10]), this can bring problems with the filters that are computationally less efficient. Because of this, to verify a "generality" of our approach, we have obtained the results for the well-known local statistic Lee filter, which is computationally efficient.

General approach to prediction

In general, our approach to prediction of filtering efficiency consists in the following. First, we assume that there is a metric that can more or less adequately characterize a filtering efficiency. This can be improvement of peak signal-to-noise ratio (IPSNR) or improvement of some other metric calculated as a difference of metric values after and before filtering. Here we do not discuss which metric is the most adequate for characterizing despeckling efficiency (to the best of our knowledge, such studies have not been carried out yet). Second, we assume that there are input parameters (one, a few or several) which are able to characterize an input image and noise in it. Third, it is supposed that there is a quite strict dependence (approximation, connection) between output parameter (metric) and input parameters. This dependence can be expressed in different ways: as some function or as some approximator (for example, support vector machine or neural network). In any case, having determined input parameters for a given image, it becomes possible to estimate (predict) the output metric. The dependence is obtained off-line and is available to a moment when the predictor has to be applied to a given image.

Having this general schedule, it becomes clear what are requirements to our predictor [10, 17]. It should be simple and and efficiently implementable, to perform a prediction faster than the filtering. This means that the number of input parameters has to be small and they shall be calculated quickly. This also means that the approximator part should perform in a fast way too. The predictor should provide an appropriate accuracy. Since different metrics vary in different ranges, an appropriate accuracy for each metric should be defined individually. As a particular case, for metrics expressed in dB as IPSNR, a predicted value has to differ from the corresponding true value by not more than 1 dB to make a prediction reasonable.

Let us explain why we propose to use the neural network as an approximator in our prediction. First, it has been shown that the use of several input parameters provides better accuracy of prediction than the use of one or two input parameters [10, 16] and, in such a situation, neural networks can be a good solution to solve the approximation task. Second, the dependences are nonlinear and this is one more argument in favor of using the NN. Third, different input parameters have different impact on accuracy of prediction and NN training is a good way to exploit positive features with input parameters (to combine them). Fourth, for SAR images (and, in particular, for Sentinel-1 SAR images), we deal with spatially correlated noise and its properties have to be taken into account by some input parameters. Having a trained NN, input parameters of different origin can be combined. Also note that statistical and spatial spectral (correlation) properties of speckle can be estimated blindly [24, 25] or interactively by analyzing homogeneous image regions in SAR images (Fig. 1).

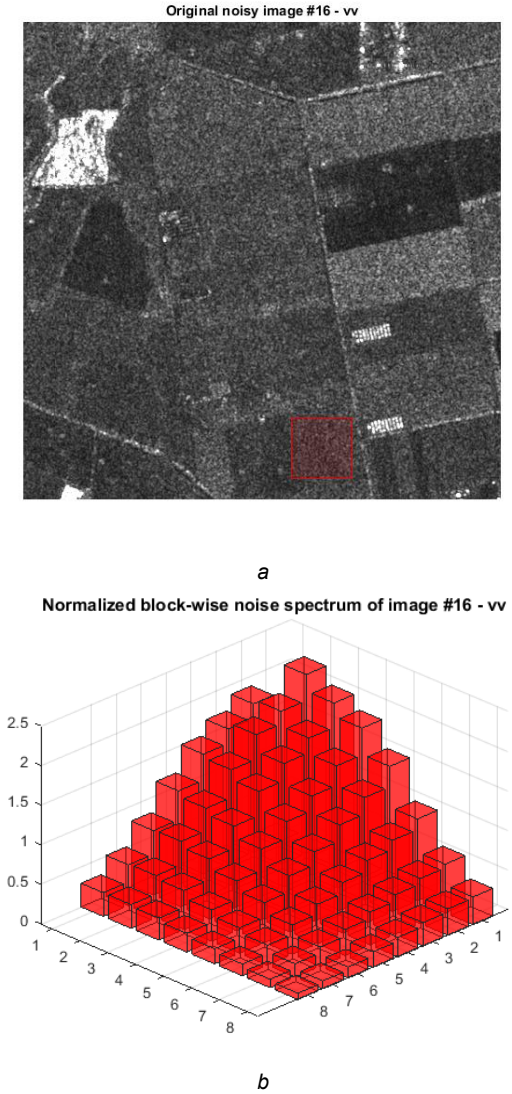

Figure 1. A fragment of Sentinel-1 SAR image with marked homogeneous region (a) and normalized spatial 8x8 DCT-spectrum (b) for VV (vertical-vertical) polarization

In a design of the NN-based predictor for the local statistic Lee filter, we employed the same approach as in [10] related to a choice of the input parameters, NN training, used metrics and criteria of their prediction accuracy, validation and verification of training results. Let us briefly consider the peculiarities of NN training.

The following metrics have been considered:

1) Conventional PSNR and visual quality metric PSNR-HVS-M [26], the latter one takes into account two important peculiarities of human vision system (HVS); note that both metrics are expressed in dB where larger values correspond to better quality;

2) Several visual quality metrics that are modifications of the known metric SSIM: FSIM [27], MS-SSIM [28], IW-SSIM [29], ADD-SSIM [30], ADD-GSIM [30], SSIM4 [31]; all these metrics vary from 0 to 1, where larger values correspond to a higher visual quality;

3) One of the best visual quality metric WSNR [32], it is expressed in dB and its larger ones correspond to a better visual quality;

4) The recently proposed metric HaarPSI [33], it varies in the limits from 0 to 1, larger values take place for better quality images;

5) The visual quality metric GMSD [34]; this metric has positive values and its smaller relate to better visual quality;

6) The visual quality metric MAD [35]; it varies in wide limits; a smaller values correspond to a better quality;

7) The metric GSM [36] that is smaller than unity, larger values correspond to a better quality;

8) The visual quality metric DSS [37], it varies in the limits from 0 to 1, larger values relate to a better visual quality.

At the beginning, we have considered four groups of input parameters (see [10] for more details). The first group included sixteen parameters calculated in the DCT spectral domain. Normalized spectral power has been determined in four spectral areas of 8x8 pixel blocks marked by digits from 1 to 4 in Fig. 2.

0	1	1	1	1	2	2	2
1	1	1	1	2	2	2	3
1	1	1	2	2	2	3	3
1	1	2	2	2	3	3	3
1	2	2	2	3	3	3	4
2	2	2	3	3	3	4	4
2	2	3	3	3	4	4	4
2	3	3	3	4	4	4	4

Figure 2. Four spectral areas in DCT domain

Then, four statistical parameters have been determined for each normalized power spectrum area - mean, variance, skewness, and kurtosis – obtaining $M_{S1..4}$, $V_{S1..4}$, $S_{S1..4}$, $K_{S1..4}$, respectively.

Another group of input parameters relates to image statistics in 8x8 pixel blocks. These are parameters M_{BM}, V_{BM}, S_{BM}, K_{BM} – the mean, variance, skewness, and kurtosis of block means, respectively.

The third group of parameters has already recommended itself in prediction of filtering efficiency well [18]. We propose to estimate probabilities $P_\sigma(q), q = 1,...,Q$ in a q-th block (Q is the total number of analyzed blocks) that absolute values of DCT

coefficients in 8x8 pixel blocks do not exceed frequency and signal-dependent thresholds:

$$T_{q\,kl} = \sigma_\mu \bar{I}_q \sqrt{D_{pn}(k,l)}\,, \quad (1)$$

where $D_{pn}(k,l)$ is the DCT power spectrum, $\bar{I}_q$ is the q-th block mean, σ_μ^2 denotes the relative variance of speckle. Having estimated $P_\sigma(q), q = 1,...,Q$, mean, variance, skewness and kurtosis of these sets are calculated and used as input parameters. They are denoted as M_P, V_P, S_P, K_P, respectively.

It was also expected in [10] that entire image statistics can be useful in predicting image filtering efficiency. Hence, a set of four parameters has been obtained: image mean, variance, skewness, and kurtosis. They are denoted as M_I, V_I, S_I, K_I, respectively.

Here we do not consider which parameters are more or less informative. Some preliminary analysis has been made in [10]. It has been shown that the use of 13 parameters (features) provides high accuracy without losing prediction performance compared to the use of all 28 input parameters. The established set of parameters includes the following ones: M_{S1}, M_{S2}, M_{S3}, M_{S4}, M_{BM}, V_{BM}, S_{BM}, M_P, V_P, S_P, K_P, M_I and V_I (the description of these parameters is given above). Thus, here we employed this set of 13 parameters to perform a prediction.

Now let us recall radar image model and give a brief description of the local statistic Lee filter. The radar image model is described as:

$$I^n(i,j) = I^{true}(i,j) \cdot \mu(i,j)\,, \quad (2)$$

where $I^n(i,j)$ is the ij-th noisy image pixel, $I^{true}(i,j)$ is the ij-th true image pixel, $\mu(i,j)$ is a Gamma distributed random variable with mean equal to unity and relative variance σ_μ^2 modeling the speckle. Note that for Sentinel-1 SAR data an estimated relative variance σ_μ^2 is about 0.05 [10].

The Lee filter output is defined as

$$I_{ij}^{Lee} = \bar{I}_{ij} + \frac{\sigma_{ij}^2}{\bar{I}_{ij}^2\sigma_\mu^2 + \sigma_{ij}^2}\left(I_{ij} - \bar{I}_{ij}\right), \quad (3)$$

where I_{ij}^{Lee} is the despeckled image, $\bar{I}_{ij}$ is the mean in the window centered on ij-th pixel, I_{ij} is the center element in the window, σ_{ij}^2 is the variance of the pixels in the window. In our study, we have used the scanning window of size 5x5 pixels.

Peculiarities of NN training

Prediction of metrics that characterize efficiency of radar image despeckling by the Lee filter is carried out using multilayer perceptrons (MLPs). For each of the considered metrics prediction, MLPs have been trained separately. The MLP-based predictor comprises three hidden layers. All hidden layers are activated through hyperbolic tangent (tanh) activation function. Linear activation function is used for the output layer. The architecture of used MLPs is shown in Fig. 3. The inputs of MLP are 13 parameters (listed above) calculated for a given original radar image. The output of MLP is one of the considered quality metrics. The MLP-based predictor has been trained using Bayesian regularization backpropagation for 30 epochs to avoid overfitting.

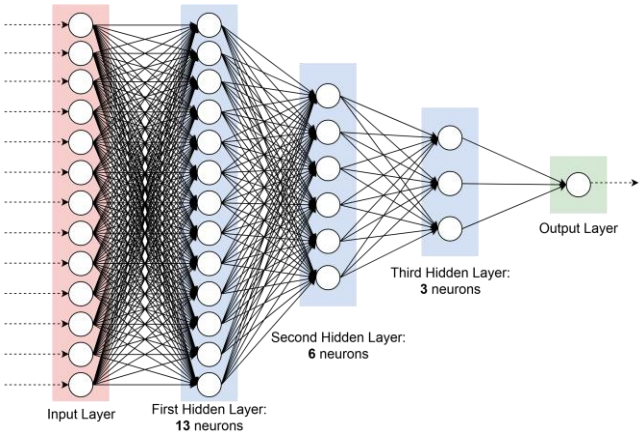

Figure 3. Architecture of used multilayer perceptron

A prediction performance of trained models has been evaluated in two stages. The first stage is so-called self-dataset validation. In this case, whole image dataset has been split into training and validation subsets (in the percentage ratio 80:20). At the next stage, cross-dataset evaluation has been applied to assess the generalization capability of trained models. According to this, MLPs have been evaluated on images that have not been involved in the training.

Testing results

After training, the NN predictor has been applied to noisy test images to verify the accuracy. In the case of regression, it is common [38] to use the following two characteristics of accuracy: root mean square error (RMSE) calculated between predicted and true values of a considered metric (RMSE has to be as small as possible) and adjusted goodness-of-the-fit R^2 that should tend to unity.

As it has been already mentioned above, we needed some practically noise-free images to add speckle to them and to process. For this purpose, 100 high-quality cloudless large size multispectral images acquired by Sentinel-2 sensor have been used. More in detail, component images in #5 and #11 channels (subbands) of multispectral data have been exploited. It is worth noting that estimated values of PSNR for images from these two channels are about 50 dB that relates to high visual quality. Standard 512x512 size images cropped from original large size component images have been analyzed. Totally, 8100 such test images from each of two channels have been studied.

It has been found that training results differ for different realizations. To analyze how stable is a training, we have also determined standard deviation (STD) of RMSE and standard deviation of adjusted R^2. These parameters have been calculated for 1000 realizations of training.

Let us start our analysis from self-dataset validation in the same channel (namely, channel #5). Recall that we present statistics for improvements of the considered metrics (for some metrics, improvement means that the corresponding metric decreases). Then, I-MS-SSIM means improvement of MS-SSIM. To get validation data, the considered dataset has been divided into two parts: 80% of images were used for training while 20% of images were employed for validation.

Analysis of data presented in Table 1 for self-dataset validation shows the following. Values of adjusted R^2 is high or very high for practically all metrics. There are some metrics (PSNR, PSNR-HVS-M, GSM, MS-SSIM, WSNR) the values of R^2 exceed 0.99. Meanwhile, there are metrics (like MAD) for which R^2 is not so large. The values of STD of adjusted R^2 are mostly small, i.e. NN training is quite stable.

RMSE values for metrics expressed in dB (PSNR, PSNRHVSM, WSNR) are small, i.e. prediction is very accurate. For metrics that vary in the limits from 0 to 1, RMSE values are also small, i.e. these metrics can be predicted accurately as well. The values of the corresponding STD of RMSE are also small.

Let us consider now the results for cross-dataset evaluation for the same channel (#5) presented in Table 2. Here, original large size component images have been divided in the aforementioned proportion, i.e. training has been carried using 80 randomly selected original large size component images and validation has been performed on the remaining 20 component images.

Then before starting processing, all large size component images have been divided into images of size 512x512. Thus, different images have been used in training and validation. Necessity of cross-validation is explained by the known fact that sometimes performance of trained NNs occurs considerably worse if they are trained for one set of data and used for another dataset with slightly different properties.

The first cross-validation stage has been performed by training carried out on 6480 test images. Prediction accuracy has been determined on other 1620 images. Analysis of data in Table 2 show that the results (compared to data in Table 1) become worse. Adjusted R^2 values have reduced a little, RMSE values have increased. STD of RMSE and adjusted R^2 have increased as well. Meanwhile, prediction accuracy is still high since adjusted R^2 for most metrics exceed 0.95.

Table 1. Characteristics of prediction for self-dataset validation in the same channel (#5)

Output parameters	RMSE	STD of RMSE	Adjusted R^2	STD of adjusted R^2
I-PSNR	0.164	'0.031'	'0.992'	'0.004'
I-PSNRHVSM	'0.120'	'0.023'	'0.992'	'0.004'
I-FSIM	'0.006'	'0.002'	'0.989'	'0.032'
I-MSSSIM	'0.004'	'0.000'	'0.997'	'0.001'
I-GMSD	'0.004'	'0.001'	'0.963'	'0.025'
I-HaarPSI	'0.008'	'0.001'	'0.972'	'0.010'
I-GSM	'0.001'	'0.001'	'0.994'	'0.045'
I-SSIM4	'0.010'	'0.002'	'0.990'	'0.004'
I-MAD	'2.852'	'0.266'	'0.863'	'0.025'
I-IWSSIM	'0.008'	'0.001'	'0.979'	'0.006'
I-ADDSSIM	'0.001'	'0.000'	'0.924'	'0.012'
I-ADDGSIM	'0.001'	'0.000'	'0.890'	'0.013'
I-DSS	'0.013'	'0.001'	'0.968'	'0.005'
I-WSNR	'0.065'	'0.011'	'0.991'	'0.004'

Table 2. Cross-dataset evaluation in the same channel (#5)

Output parameters	RMSE	STD of RMSE	Adjusted R^2	STD of adjusted R^2
I-PSNR	'0.183'	'0.036'	'0.989'	'0.006'
I-PSNRHVSM	'0.135'	'0.028'	'0.988'	'0.008'
I-FSIM	'0.007'	'0.001'	'0.987'	'0.004'
I-MSSSIM	'0.005'	'0.001'	'0.996'	'0.002'
I-GMSD	'0.005'	'0.001'	'0.951'	'0.013'
I-HaarPSI	'0.009'	'0.002'	'0.961'	'0.020'
I-GSM	'0.001'	'0.000'	'0.995'	'0.002'
I-SSIM4	'0.011'	'0.002'	'0.987'	'0.007'
I-MAD	'3.115'	'0.726'	'0.819'	'0.085'
I-IWSSIM	'0.009'	'0.002'	'0.968'	'0.022'
I-ADDSSIM	'0.001'	'0.000'	'0.905'	'0.031'
I-ADDGSIM	'0.001'	'0.000'	'0.863'	'0.058'
I-DSS	'0.015'	'0.003'	'0.955'	'0.034'
I-WSNR	'0.070'	'0.014'	'0.987'	'0.009'

Table 3. Cross-dataset evaluation using another channel (#11)

Output parameters	RMSE	STD of RMSE	Adjusted R^2	STD of adjusted R^2
I-PSNR	'0.319'	'0.077'	'0.949'	'0.029'
I-PSNRHVSM	'0.262'	'0.077'	'0.935'	'0.044'
I-FSIM	'0.009'	'0.001'	'0.976'	'0.008'
I-MSSSIM	'0.007'	'0.001'	'0.988'	'0.008'
I-GMSD	'0.007'	'0.001'	'0.871'	'0.049'
I-HaarPSI	'0.014'	'0.004'	'0.869'	'0.069'
I-GSM	'0.001'	'0.000'	'0.990'	'0.005'
I-SSIM4	'0.013'	'0.003'	'0.974'	'0.012'
I-MAD	'4.772'	'0.995'	'0.349'	'0.247'
I-IWSSIM	'0.010'	'0.002'	'0.939'	'0.030'
I-ADDSSIM	'0.002'	'0.000'	'0.790'	'0.091'
I-ADDGSIM	'0.002'	'0.000'	'0.733'	'0.092'
I-DSS	'0.019'	'0.004'	'0.895'	'0.049'
I-WSNR	'0.156'	'0.055'	'0.917'	'0.062'

Finally, cross-dataset evaluation has been done using images of another channel (#11) in the following way: 80 large size component images from the #5 channel have been taken for training and remaining 20 images from the #11 channel have been used to evaluate prediction performance. The results are presented in Table 3. Comparison of the corresponding values in Table 3 to data in Tables 1 and 2 shows that prediction accuracy becomes worse – Adjusted R^2 decreases, RMSE and standard deviations increase. However, for most metrics the prediction accuracy is still at a desired level.

Conclusions

The paper deals with NN-based prediction of metrics that characterize efficiency of radar images denoising by the local statistic Lee filter. Novelty of the proposed approach and obtained results consists in the following: 1) possibility of performance prediction for the Lee filter is shown; 2) neural network is trained for this purpose with application to Sentinel-1 data; 3) a set of good input parameters is obtained; 4) methodology of NN training for a particular application and validation results are presented.

It is demonstrated that for most metrics including visual quality ones accuracy of prediction is quite high. This means that our approach proposed in [10] is quite general. In the future, we plan to consider other filters and SAR images with other properties.

REFERENCES

[1] J.-S. Lee, E. Pottier, "Polarimetric Radar Imaging: From Basics to Applications," CRC Press, 2009, 422 p.

[2] N. Kussul, S. Skakun, A. Shelestov, and O. Kussul, "The use of satellite SAR imagery to crop classification in Ukraine within JECAM project," in Proc. IEEE International Geoscience and Remote Sensing Symposium (IGARSS), 2014, pp. 1497-1500.

[3] A. G. Mullissa, C. Persello, and V. Tolpekin, "Fully Convolutional Networks for Multi-Temporal SAR Image Classification," in Proc. IEEE International Geoscience and Remote Sensing Symposium (IGARSS), 2018, pp. 6635-6638.

[4] R. A. Touzi, "Review of Speckle Filtering in the Context of Estimation Theory," IEEE Trans. on GRS, vol. 40, no. 11, pp. 2392-2404, 2002.

[5] C. Oliver, S. Quegan, "Understanding Synthetic Aperture Radar Images", SciTech Publishing, 2004, 486 p.

[6] P. Kupidura, "Comparison of Filters Dedicated to Speckle Suppression in SAR Images," ISPRS-International Archives of the Photogrammetry, Remote Sensing and Spatial Information Sciences, pp. 269-276, 2016.

[7] S. Solbo, T. Eltoft, "A stationary wavelet domain Wiener filter for correlated speckle," IEEE Transactions on Geoscience and Remote Sensing, vol.46, no 8, pp. 1219-1230, 2008.

[8] C.A. Deledalle, L. Denis, S. Tabti, F. Tupin, "MuLoG, or how to apply Gaussian denoisers to multi-channel SAR speckle reduction?," IEEE Transactions on Image Processing, vol. 26, no. 9, pp. 4389-4403, 2017.

[9] M. Makitalo, A. Foi, D. Fevralev, V. Lukin, "Denoising of single-look SAR images based on variance stabilization and non-local filters," in Proc. of MMET, Kiev, Ukraine, Sept. 2010, pp. 1-4.

[10] O. Rubel, V. Lukin, A. Rubel, K. Egiazarian, "NN-Based Prediction of Sentinel-1 SAR Image Filtering Efficiency," Geosciences, vol. 9, no. 7, 22 p., 2019.

[11] S. Abdikan, F.B. Sanli, M. Ustuner, F. Calò, "Land Cover Mapping Using Sentinel-1 SAR Data," in Proceedings of ISPRS - International Archives of the Photogrammetry, Remote Sensing and Spatial Information Sciences, June 2016, Prague, Czech Republic, pp. 757-761.

[12] T. Whelen, P. Siqueira, "Time-series classification of Sentinel-1 agricultural data over North Dakota," Remote Sensing Letters, vol. 9, no. 5, pp. 411-420, 2018.

[13] P. Ye, J. Kumar, L. Kang, and D. Doermann, "Unsupervised feature learning framework for no-reference image quality assessment," in Proc. IEEE Conference on Computer Vision and Pattern Recognition, 2012, pp. 1098–1105.

[14] S. Bosse, D. Maniry, K. R. Muller, T. Wiegand, and W. Samek, "Deep neural networks for no-reference and full-reference image quality assessment," IEEE Trans. Image Process., vol. 27, no. 1, pp. 206-219, Jan. 2018.

[15] L. Gomez, R. Ospina, A.C. Frery, "Statistical Properties of an Unassisted Image Quality Index for SAR Imagery," Remote Sensing, vol. 11, pp. 1-16, 2019.

[16] O. Rubel, V. Lukin, "An Improved Prediction of DCT-Based Filters Efficiency Using Regression Analysis," Information and Telecommunication Sciences, vol. 5, no. 1, Kiev, Ukraine, pp. 30-41, 2014.

[17] O. Rubel, V. Lukin, S. Abramov, B. Vozel, O. Pogrebnyak, and K. Egiazarian, "Is Texture Denoising Efficiency Predictable?," International Journal of Pattern Recognition and Artificial Intelligence, vol. 32, no. 01, p. 32, 2018.

[18] O.S. Rubel, V.V. Lukin. F.S. de Medeiros, "Prediction of Despeckling Efficiency of DCT-based filters Applied to SAR Images," in Proceedings of DCOSS, Fortaleza, Brazil, June 2015, pp. 159-168.

[19] M. A. Saad, A. C. Bovik and C. Charrier, "Model-Based Blind Image Quality Assessment: A natural scene statistics approach in the DCT domain," IEEE Transactions Image Processing, vol. 21, no. 8, pp. 3339-3352, 2012.

[20] D. M. Chandler, "Seven Challenges in Image Quality Assessment: Past, Present, and Future Research," ISRN Signal Processing, vol. 2013, pp. 1-53, 2013.

[21] A. K. Moorthy and A. C. Bovik, "A Two-Step Framework for Constructing Blind Image Quality Indices," in IEEE Signal Processing Letters, vol. 17, no. 5, pp. 513-516, May 2010.

[22] V. Lukin, S. Abramov, S. Krivenko, A. Kurekin, O. Pogrebnyak, "Analysis of classification accuracy for pre-filtered multichannel remote sensing data," Journal of Expert Systems with Applications, vol. 40, pp. 6400-6411, 2013.

[23] J. Lee, "Digital Image Enhancement and Noise Filtering by Use of Local Statistics," in IEEE Transactions on Pattern Analysis and Machine Intelligence, vol. PAMI-2, no. 2, pp. 165-168, March 1980.

[24] M. Colom, M. Lebrun, A. Buades, J.-M. Morel, "Nonparametric multiscale blind estimation of intensity-frequency-dependent noise," IEEE Transactions on Image Processing, vol. 24, no 10, pp. 3162-3175, 2015.

[25] M. Uss, B. Vozel, V. Lukin, K. Chehdi, "Maximum Likelihood Estimation of Spatially Correlated Signal-Dependent Noise in Hyperspectral Images," Optical Engineering, vol. 51, no. 11, 2012.

[26] N. Ponomarenko, F. Silvestri, K. Egiazarian, M. Carli, J. Astola, and V. Lukin, "On between-coefficient contrast masking of DCT basis functions," in Proc. 3rd Int. Workshop Video Process. Qual. Metrics Consum. Electron, Scottsdale, USA, Jan. 2007, 4 p.

[27] L. Zhang, L. Zhang, X. Mou, and D. Zhang, "FSIM: A feature similarity index for image quality assessment," IEEE Trans. Image Process., vol. 20, no. 8, pp. 2378–2386, Aug. 2011.

[28] Z. Wang, E. P. Simoncelli, and A. C. Bovik, “Multi-scale structucal similarity for image quality assessment,” in Proc. IEEE 37th Asilomar Conf. Signals, Syst., Comput., Pacific Grove, CA, Nov. 2003, pp. 1398-1402.

[29] Z. Wang and Q. Li, “Information content weighting for perceptual image quality assessment,” IEEE Trans. Image Process., vol. 20, no. 5, pp. 1185-1198, May 2011.

[30] K. Gu, S. Wang, G. Zhai, W. Lin, X. Yang, and W. Zhang, “Analysis of Distortion Distribution for Pooling in Image Quality Prediction,” IEEE Transactions on Broadcasting, vol. 62, no. 2, pp. 446-456, 2016.

[31] M. Ponomarenko, K. Egiazarian, V. Lukin, and V. Abramova, “Structural Similarity Index with Predictability of Image Blocks,” in Proceedings of International Conference MMET 2018, July 2-5, 2018, 4p.

[32] T. Mitsa and K. Varkur, “Evaluation of contrast sensitivity functions for the formulation of quality measures incorporated in halftoning algorithms,” in Proc. IEEE International Conference on Acoustics Speech and Signal Processing, vol. 5, Apr. 1993, pp. 301-304.

[33] R. Reisenhofer, S. Bosse, G. Kutyniok, and T. Wiegand, “A Haar Wavelet-Based Perceptual Similarity Index for Image Quality Assessment,” Signal Processing: Image Communication, vol. 61, pp. 33-43, Feb. 2018.

[34] W. Xue, L. Zhang, X. Mou, and A. C. Bovik, “Gradient magnitude similarity deviation: A highly efficient perceptual image quality index,” IEEE Trans. Image Process., vol. 23, no. 2, pp. 684–695, Feb. 2014.

[35] E.C. Larson and D.M. Chandler, “Most apparent distortion: Full-reference image quality assessment and the role of strategy,” J. Electron. Imagining, vol. 19, no. 1, pp. 011006:1-011006:21, 2010.

[36] A. Liu, W. Lin, and M. Narwaria, “Image quality assessment based on gradient similarity,” IEEE Trans. Image Process., vol. 21, no. 4, pp. 1500–1512, Apr. 2012.

[37] A. Balanov, A. Schwartz, Y. Moshe, and N. Peleg, “Image quality assessment based on DCT subband similarity,” in Proc. IEEE Int. Conf. Image Process. (ICIP), 2015, pp. 2105-2109.

[38] A.C. Cameron and F. Windmeijer, “An R-squared measure of goodness of fit for some common nonlinear regression models,” Journal of Econometrics, vol. 77, no. 2, pp. 329-342, April 1997.

JOIN US AT THE NEXT EI!

IS&T International Symposium on

Electronic Imaging

SCIENCE AND TECHNOLOGY

Imaging across applications . . . Where industry and academia meet!

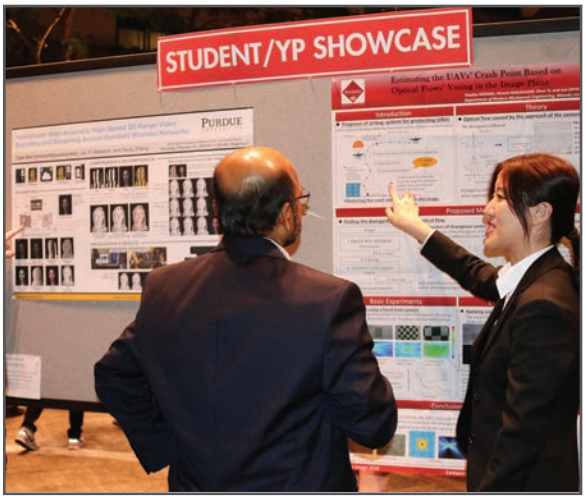

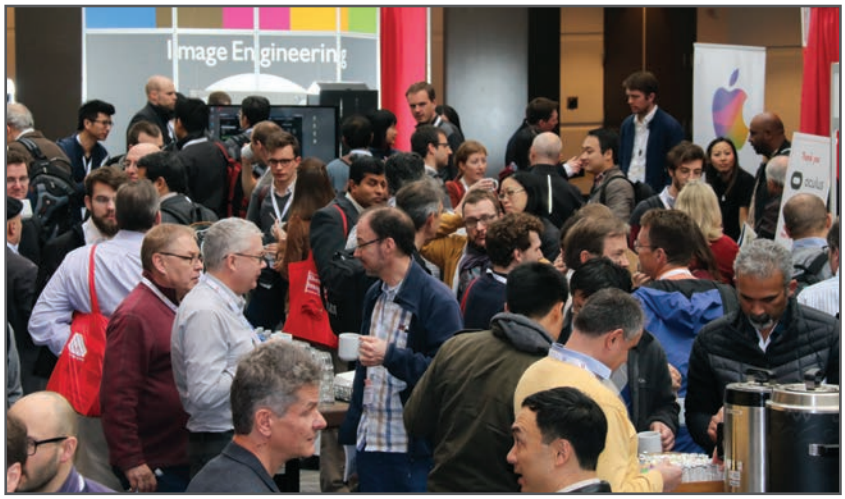

• SHORT COURSES • EXHIBITS • DEMONSTRATION SESSION • PLENARY TALKS •
• INTERACTIVE PAPER SESSION • SPECIAL EVENTS • TECHNICAL SESSIONS •

www.electronicimaging.org

IS&T
imaging.org